STOCHASTIC BIFURCATION ON THE IMPACT PROBLEM BETWEEN TWO ELASTIC BODIES

Fernando S. Buezas[a,b], Marta B. Rosales[b,c] and Rubens Sampaio[d]

[a]*Departamento de Física, Universidad Nacional del Sur, Av. Alem 1253, (8000) Bahía Blanca, Argentina, fbuezas@gmail.com*

[b]*CONICET, Argentina*

[c]*Departamento de Ingeniería, Universidad Nacional del Sur, Av. Alem 1253, (8000) Bahía Blanca, Argentina, mb.rosales55@gmail.com*

[d]*PUC-Rio, Department of Mechanical Engineering, Rua Marquês de São, 225, Gávea, RJ, 22453-900, Brazil, rsampaio@puc-rio.br*

Keywords: uncertainty, contact, elastic problem, multimodality, stochastic modeling

Abstract. An uncertainty quantification study is carried out in the problem of frontal collision of two elastic bodies. The time of contact and the resultant force function involved during the collision are the quantities of interest. If the initial conditions and the mechanical and geometrical properties were known, the response prediction would be deterministic. However, if the data contains any uncertainty, a stochastic approach becomes appropriate. Based on the Principle of Maximum Entropy (PME), and under certain restrictions on the parameter values, we derive the probability density function (PDF) for each of the stochastic parameters to construct a probabilistic model. Two cases are dealt with: one of a collision involving two spheres and another of the collision of two discs. In the first case, a parameter involving geometry and material properties is assumed stochastic. Since an analytical model exists, the propagation of the uncertainty of the time of contact can be done analytically. However, the interaction force function can only be computed from the solution of a nonlinear ordinary differential equation, hence not analytically. Given the PDF of the parameter, the problem of uncertainty propagation is tackled using Monte Carlo simulations. The comparison of both approaches yields an excellent agreement. With respect to the collision of two discs, first the small deformation problem, within the Hertz theory, is addressed with a Monte Carlo method. When the discs undergo large deformations, the problem is approximated using the equations of Finite Elasticity discretized by the finite element method (FEM) and combined with a Monte Carlo simulations. In a first illustration, the modulus of elasticity is assumed stochastic with a gamma PDF. Further, the disc collision problem is analyzed when two parameters are stochastic: the modulus of elasticity and the Poisson's ratio. It is shown that under certain dispersion ranges, the PDF of the interaction force function undergoes a qualitatively change exhibiting bimodality.

1 INTRODUCTION

The collision among solid bodies involves magnitudes such as the time of contact and interaction forces which are not easily obtained from physical measurements due to the complexity of this phenomenon (Hessel et al., 2006). In a very small time, large forces are developed in a frontal collision between elastic bodies (Buezas et al., 2010). The interest in collision problems is quite old (Timoshenko, 1913), some articles deals with rigid-body collisions (Cataldo and Sampaio, 2000, 2001b,a, 2002), discrete systems (Sampaio and Tavares, 1998), continuous systems (Sampaio and Soize, 2007; Ritto et al., 2012). For collision of deformable bodies some books have appeared (Johnson, 1985; Popov, 2010; Stronge, 2000).

Recently, Langley (2012) reports a study on the the characteristics of the interaction force function produced when two randomly vibrating elastic bodies colliding with each other, or when a single randomly vibrating elastic body collides with a barrier. On the other hand, when dealing with mechanical models, uncertainties are always present and taking them into account improves model predictability (Ritto et al., 2011; Pagnacco et al., 2011). This paper deals with the quantification of the uncertainties on some of the mechanical properties of elastic bodies undergoing frontal elastic-collision and their propagation to the time of contact and the interaction force function during the collision. Of course, in colliding elastic bodies one deals with stress fields, but in this paper the resultant force in the direction of the frontal collision is computed and one studies its variation during the collision, that is one studies a stochastic process. In particular, the study is focused on the collisions of spheres and discs. First, the collision of two spheres within the well-known Hertz theory (Landau and Lifchitz, 1969; Johnson, 1985) is tackled. Due to the simple function that relates the time of contact and the impact speed in this particular case, the uncertainty problem is solved analytically. The analytical solution is also compared with stochastic simulations. Second, a similar problem involving discs is approximated through statistical tools. One or two parameters are assumed stochastic and the propagation of the uncertainty is studied using a probabilistic models derived by the Principle of Maximum Entropy.

The article is organized as follows. First, a variable that includes geometric and material properties of the two sphere collision problem is assumed stochastic and the PDF deduced from the Principle of Maximum Entropy (PME) (Shannon, 1948). Making use of the theorem regarding a change of variable, the PDF of the time of contact is analytically derived. The parameters of the PDF found with the PME can be adjusted with experimental data reported in Hessel et al. (2006). The PDFs of the time of contact and the interaction force function (evolution of the interaction force during the collision process) are predicted when the speed of the collision is varied. Afterwards, the same problem is approximated making use of stochastic simulations. It was found that both, the analytic and the computational approaches, yield similar results. It follows a section dealing with an analogous problem that involves the collision of two elastic discs. Here, the Hertz model is compared with a finite elasticity solution for both low and high speed collisions using the equations of Finite Elasticity discretized by finite elements. In this case, there is no explicit relationship between the time of contact τ and impact speed v neither in the Hertz model nor in the Finite Elasticity solution. Hence, the analytical approach is not feasible and a numerical procedure was the alternative. Two cases are discussed. In one case, the modulus of elasticity is assumed as a statistic variable with a gamma PDF. The propagation of the uncertainty yields the PDFs of the time of contact and interaction force. In the other case, two parameters are varied simultaneously, the modulus of elasticity and the Poison's coefficient. The first parameter is represented by a gamma PDF and the second one,

by a uniform PDF. Also, the influence of the dispersion value is assessed. The evolution of PDF of the interaction force function exhibits changes from unimodality to bimodality, and even multimodality, making evident the complexity of the problem. Finally, some comments are included and some works in progress are described.

2 COLLISION BETWEEN SPHERES. STATEMENT OF THE PROBLEM

The time of contact, τ, between two colliding spheres in function of the collision speed, v, when small deformations are assumed, is given by (Landau and Lifchitz, 1969; Hessel et al., 2006),

$$\tau = \alpha v^{\gamma} \tag{1}$$

where α and γ are parameters. Within the Hertz theory, they assume the following values

$$\alpha = 2.94 \sqrt[5]{\frac{\mu_m^2}{k^2}}; \quad \gamma = -\frac{1}{5} \tag{2}$$

in which the reduced mass is $\mu_m = m \, m'/(m + m')$, $k = 4\sqrt{rr'/(r + r')}/5D$ and $D = 3\left[(1 - \nu^2)/E + (1 - \nu'^2)/E'\right]/4$. E and ν stand for the modulus of elasticity and the Poisson's ratio of each sphere, respectively, m is the mass of one sphere, and r denotes the radius of the sphere. The prime denotes the second sphere data.

Each quantity involved in the determination of α is a positive scalar which makes α also positive. One could tackle it as a positive stochastic variable. In fact, a negative value of those parameters would lead to negative time of contact which is meaningless. If a stochastic approach is applied to this problem, first a PDF should be chosen for the input variable. A statistical concept of entropy was introduced by Shannon in the theory of communication and transmission of information (Shannon, 1948). He derived the Principle of Maximum Entropy which states that, subject to known constraints, the PDF which best represents the current state of knowledge is the one with largest entropy. The measure of uncertainties of a random variable X is defined by the following expression

$$S(f_X) = - \int f_X(X) log(f_X(x)) dX \tag{3}$$

in which f_X stands for the PDF of X.

It is possible to demonstrate that the application of the principle under the contraints of positiveness and bounded second moment, leads to a gamma PDF (see for instance, Pérez (2007)) for the random variable under study. This situation applies to the variable α, *i.e.* the gamma PDF is

$$f(\alpha) = \frac{\alpha^{d-1} e^{-\alpha/b}}{b^d \Gamma(d)} \tag{4}$$

where d and b are the two parameters of the distribution that are related to the mean μ and the variance σ^2, as follows,

$$\mu = bd; \quad \sigma^2 = b^2 d. \tag{5}$$

Now, given the distribution of the parameter α, the natural question is: what are the distributions of the time of contact, a random variable, and of the interaction force function, a stochastic process (hence a distribution for each instant)? As was mentioned before, the simplicity of this problem, allows for an analytical analysis in the following sections and afterwards a comparison with a numerical approach.

2.1   Change of variable

The probability of finding a value of the random variable X, with PDF $f(X)$, between m and n is

$$P(m < X < n) = \int_m^n f(X)dX \tag{6}$$

Then, the following theorem (see, for instance, Spiegel (1998); Rubinstein (2007)) applies

Theorem 1 *Let X be a continuous random variable with PDF $f(X)$. Let us define $U = \phi(X)$ and its inverse function $X = \psi(U)$. Then, the PDF of U is given by $g(U)$ where*

$$g(U)\,|dU| = f(X)\,|dX| \tag{7}$$

or

$$g(U) = f(X)\left|\frac{dX}{dU}\right| = f(\psi(U))\,|\psi'(U)|. \tag{8}$$

The application of this theorem to the time of contact τ (see Eq. (1)) yields

$$g(\tau) = f(\alpha)\left|\frac{d\alpha}{d\tau}\right| = f\left(\frac{\tau}{v^\gamma}\right)\frac{1}{v^\gamma}. \tag{9}$$

As mentioned before, α is assumed with a gamma PDF, and consequently,

$$g(\tau) = \frac{\left(\frac{\tau}{v^\gamma}\right)^{d-1}e^{-\left(\frac{\tau}{v^\gamma}\right)/b}}{b^d\Gamma(d)v^\gamma}. \tag{10}$$

3   COLLISION BETWEEN SPHERES

In this subsection, the collision problem between two spheres will be tackled numerically. The mean data is extracted from the values of the experiment reported by Hessel et al. (2006). The case corresponds to the problem of two identical steel spheres with $2r = 2r' = 0.0381$ m, mass $m = m' = 0.2258$ kg, Poissons ratio $\nu = \nu' = 0.3$ and modulus of elasticity $E = E' = 2.1\ 10^{11}$ Pa (recall Eq. (2)). The mean value of α reported in this reference is $\mu_\alpha = (1.138)\,10^{-4}$. The standard deviation of α will be varied from a lower bound of $\sigma_\alpha = 2\ 10^{-5}$. The results are reported for an impact speed of $v = 20$ m/s.

Figure 1 shows three gamma PDFs $f(\alpha)$ for the parameter α obtained for the adopted value of the mean μ_α and three values of σ_α. After applying the change of variable technique (Eq. (10)) the PDF $g(\tau)$ of the time of contact variable τ is obtained and shown in Fig. 2. It can be observed that, for the case of $\sigma_\alpha = 2\ 10^{-5}$ both distributions $f(\alpha)$ (Fig. 1) and $g(\tau)$ show symmetry and resemble a gaussian distribution. However, it should be noted that they still keep the property of being zero when the variable is zero, which is consistent with the positive domain of the random variable. As the dispersion increases, the PDFs tend to skew to the left, getting closer to the typical gamma distributions. Recall that all the distributions $f(\alpha)$ have the same expected value $\mu_\alpha = 1.138\ 10^{-4}$. The same happens for the time of contact, resulting $\mu_\tau = 6.2508\ 10^{-5}s$ as should be expected from the relationship (1).

3.1   Variation in the impact speed and interaction force function

The above calculations were carried out with a fixed value of the impact speed. It is interesting to analyze the effect on the distribution $g(\tau)$ when the value of this speed is changed.
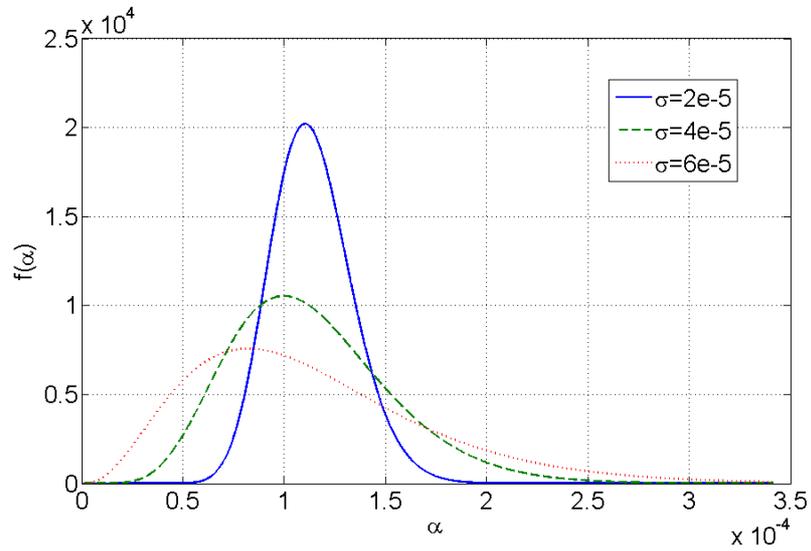
Figure 1: Gamma probability density functions for the parameter α for three values of the standard deviation σ_α.
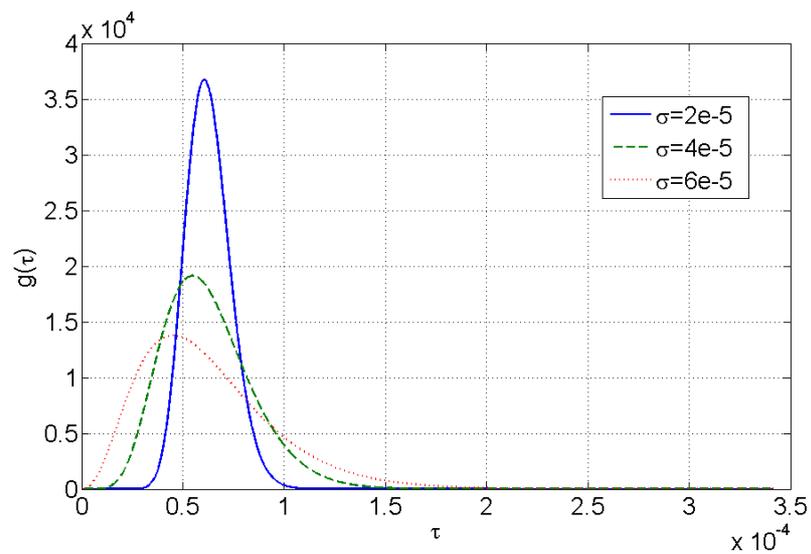

Figure 2: Probability density functions for the time of contact τ for three values of the standard deviation σ_α.
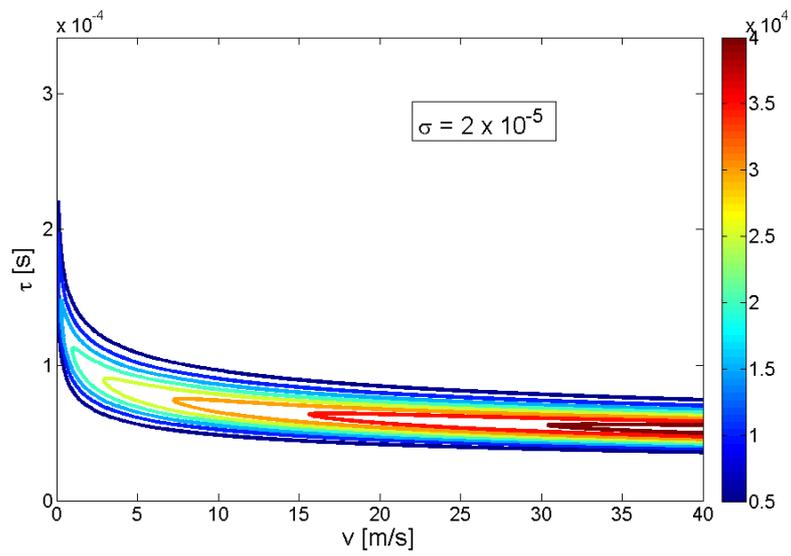
Figure 3: Collision of two steel spheres. Contour lines of the function $g(v, \tau)$ with $\sigma_\alpha = 2\ 10^{-5}$.
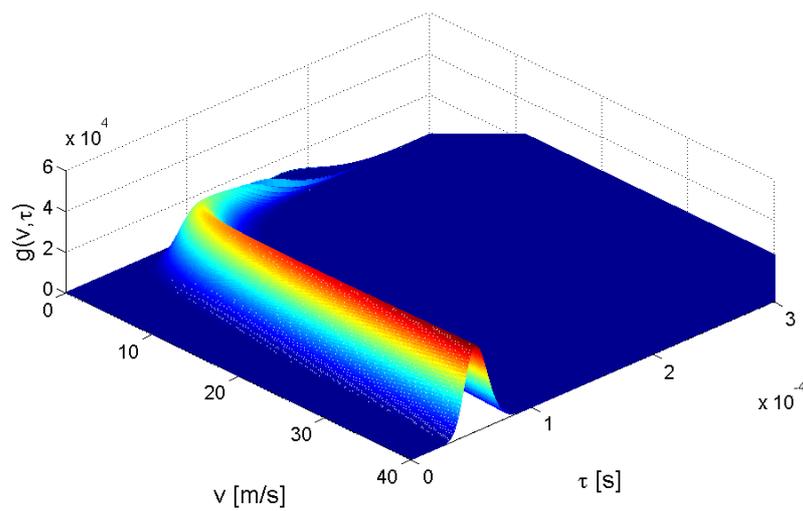

Figure 4: Collision of two steel spheres. Function $g(v, \tau)$ with $\sigma_\alpha = 2\ 10^{-5}$.
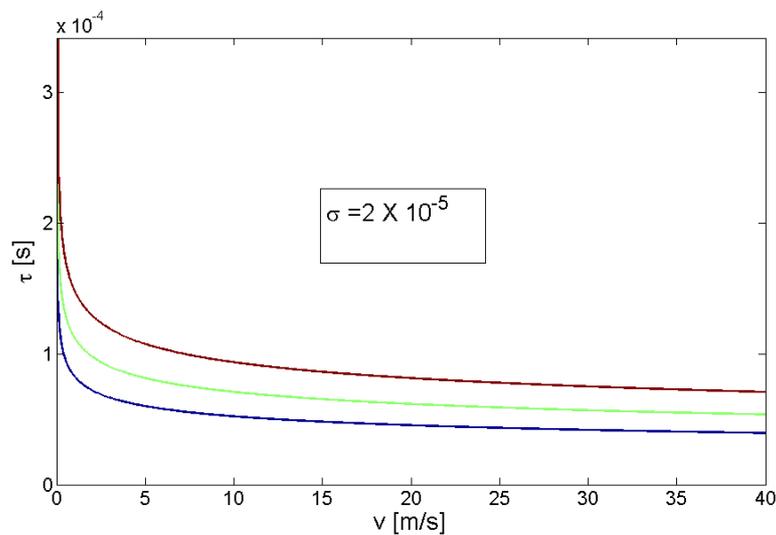
Figure 5: Curves τ vs. v and the 5% y 95% bounds for a dispersion $\sigma_\alpha = 2\ 10^{-5}$.

Figure 3 shows the contour lines of the function $g(v, \tau)$ if $\sigma_\alpha = 2\ 10^{-5}$ and Fig. 4 depicts a three dimensional graph of $g(v, \tau)$ The distribution of the time of contact τ is apparent at each cut of function $g(v, \tau)$ at a constant value of v.

Now, the cumulative probability functions can be found integrating the PDFs as follows.

$$G(z, v) = \int_0^z g(v, \tau)\, d\tau \tag{11}$$

and serve as a tool to obtain bounds and confidence intervals of the stochastic variable. For instance, if one requires an interval between the 5% and the 95% of statistical significance, the integral (11) should be evaluated as follows. For the 5% bound, x is sought such that $G(x, v) = 0.05$ and analogously with the 95% bound, x such that $G(x, v) = 0.95$. Figures 5, 6 and 7 depict the bounds corresponding to 5%, 50% y 95% of probability for the cases in which $\sigma_\alpha = 2\ 10^{-5}, 4\ 10^{-5}, 6\ 10^{-5}$, respectively.

The interaction force can be also evaluated when the parameter α is assumed random (always with a gamma distribution). It is necessary to solve the equation of motion for the interaction force between the spheres (see for instance Landau and Lifchitz (1969); Hessel et al. (2006); Puttock and Thwaite (1969)). Obviously, this interaction force and the time of contact given by Eq. (1) are related to the same problem. Figure 8 includes the temporal variation of the interaction force calculated with an impact relative velocity of 20 m/s calculated for the bounds 5%, 50% and 95% respectively, and also the mean value, in all cases with $\sigma_\alpha = 4\ 10^{-5}$. As can be observed, the latter is not coincident with the 50% bound, as would be the case if a gaussian distribution had been chosen.

4 MONTE CARLO SIMULATION AND COMPARISON WITH THE ANALYTICAL RESULT FOUND VIA THE CHANGE OF VARIABLE

Up to this point, all the results were obtained after assuming the distribution given by Eq.(4) and the change of variable of Eq.(10). The equation of motion for the same problem described in Section 3 and governed by an ordinary equation of motion is now solved. The interaction
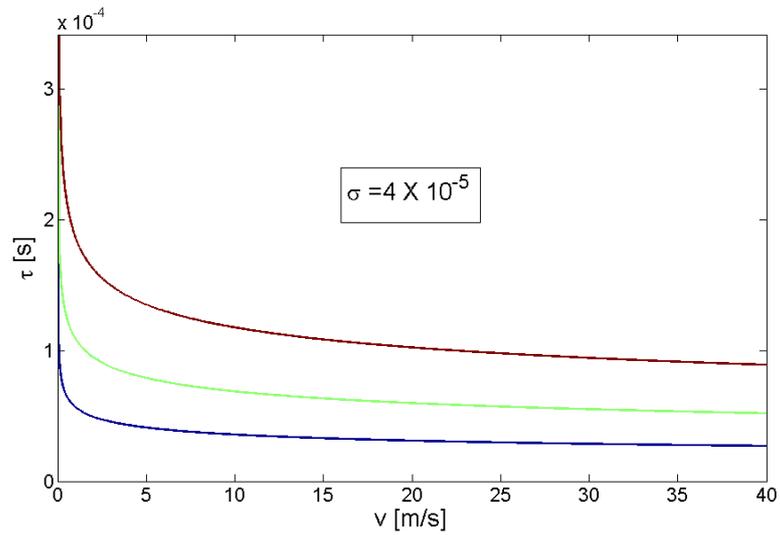
Figure 6: Curves τ vs. v and the 5% y 95% bounds for a dispersion $\sigma_\alpha = 4\ 10^{-5}$.
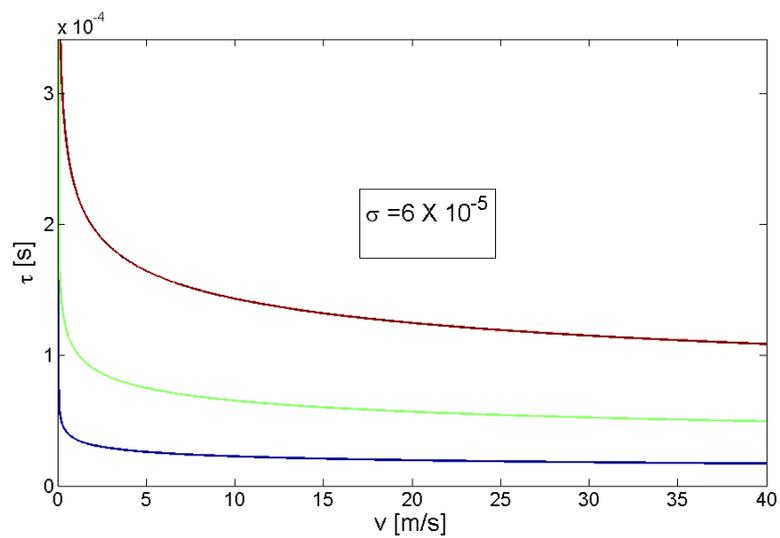

Figure 7: Curves τ vs. v and the 5% y 95% bounds for a dispersion $\sigma_\alpha = 6\ 10^{-5}$.
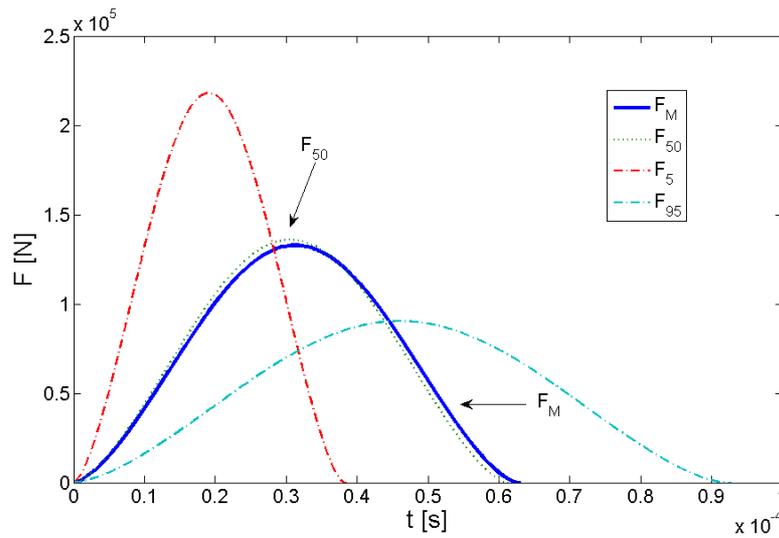
Figure 8: Impact force during contact for the bounds 5%, 50% and 95 % and the expected value F_M.

force is governed by a relationship of the type

$$F = Cx^{3/2} \tag{12}$$

where x is the separation distance between the two centers when the spheres start the collision (see e.g. Landau and Lifchitz (1969)) and C is a constant. As mentioned before, these equations derive from the equilibrium problem of elastic bodies that are in contact, stated by Hertz. In fact, the expression can be written as

$$F^{2/3} = \frac{x}{\sqrt[3]{\frac{9}{2r}\left(\frac{1-\nu^2}{E}\right)^2}} \tag{13}$$

The time of contact (Eq. (1)) is obtained from this equation combined with the second Newton's law (the reader can refer to Landau and Lifchitz (1969) for more details).

In order to verify the analytical results and to extend the methodology to other problems in which the analytical approach is not feasible, a numerical experiment was carried out. Equation (12) is approximated assuming α as a random variable and the Monte Carlo method as the stochastic solver. By the use of a random number generator that simulates the gamma distribution, the hertzian model of contact is approximated. Approximately, the number of realizations was two thousands obtained from the distribution given in Eq.(4), *i.e.* $\mu_\alpha = 1.138 \ 10^{-4}$ and $\sigma_\alpha = 0.6 \ 10^{-4}$.

Figure 9 shows the difference between the value of the dispersion σ propagated to the solution of the time of contact (numerical simulation) and the value of σ_0 obtained in the analytical evaluation (also propagated by the differential relationship $d\tau = v^\gamma d\sigma$). As can be observed, the two values of dispersion tend to match after 700 realizations, approximately. This could be a good criterion to decide the number of realizations necessary to obtain significant statistic results.

The histograms found with the 2000 realizations are shown in Fig. 10 for the parameter α and the propagation to the time of contact τ. The resemblance to the shape of the gamma distribution is apparent. It should be noted that the seesaw shape of the histograms would be smoothed if the number of bins were increased as well as the number of realizations. However,
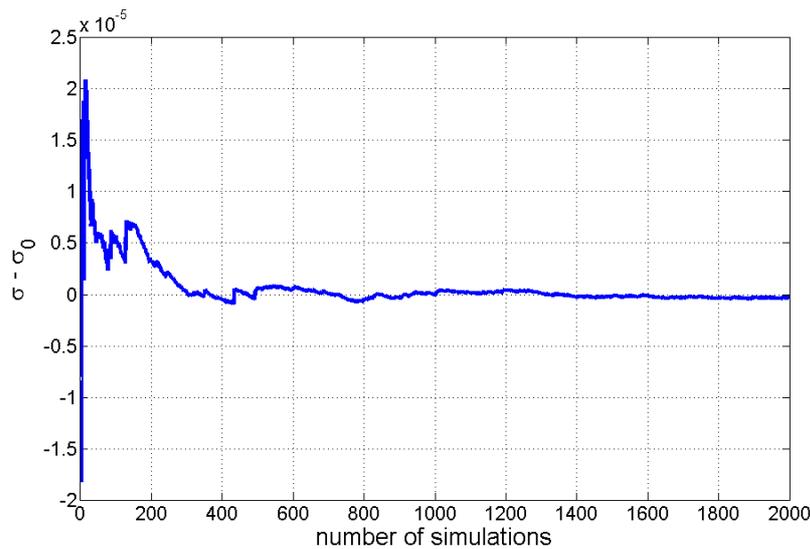
Figure 9: Collision between two spheres. Convergence study of the time of contact using the Monte Carlo method. σ and σ_0 correspond to the standard deviation found with the numerical simulation and the analytical approach, resp.
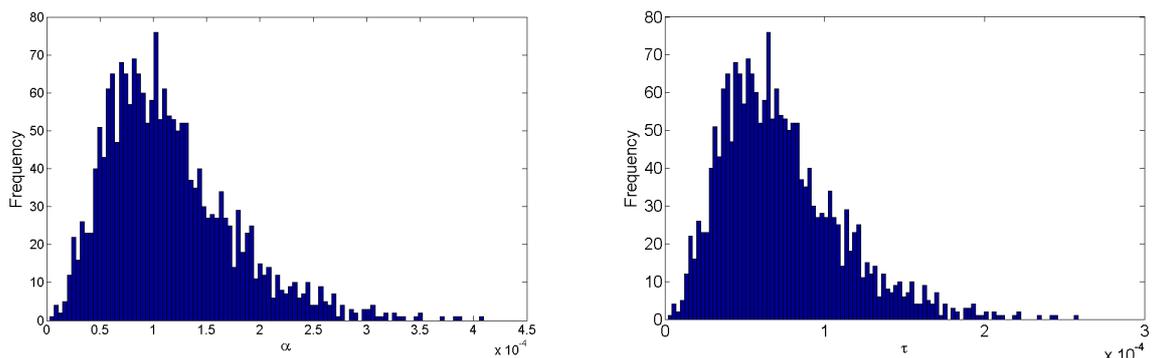

Figure 10: Collision between two spheres. Histograms found with Monte Carlo simulation and 2000 realizations. Left graph: parameter α; right graph: time of contact τ.

here the aim is to obtain a probability density estimate. The same comment applies to Figs. 13 and 15.

An interesting analysis can be done using the *ksdensity(x)* function of MATLAB that computes a probability density estimate of the sample in the vector x, *i.e.* given the results of the experiments in the form of histograms, this function yields a numerical estimate of a probability density function. Figure 11 depicts the obtained result from the previous numerical experiments via Monte Carlo simulations along with the PDFs found with the analytical approach (Eqs. (4) and (10)) using the change of variable technique.

5   COLLISIONS BETWEEN TWO DISCS

The problem of the collision of two discs is herein analyzed. The discs problem presents the advantage that it can be reduced to a 2D study. This feature will become useful when the large deformation problem is approximated regarding a drastic reduction on the computational time. With the aim of evaluating the distributions of the time of contact, a comparison of the
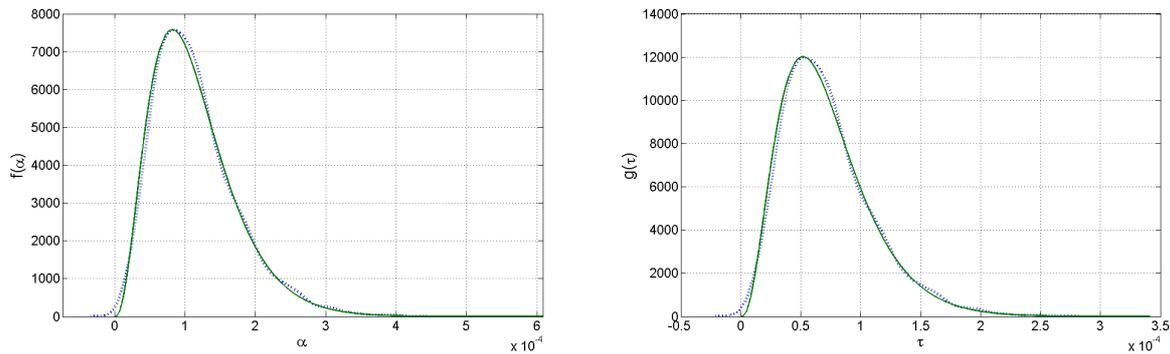
Figure 11: Collision between two spheres. Reconstruction of the PDFs from the numerical simulations using Monte Carlo method. Full lines: distributions found with the analytical approach. Dashed lines: distributions reconstructed from data of Fig. 10.

results found with the model of Eq. (13) will be compared with a nonlinear model of collision (Buezas et al., 2010) for two rubber discs. The latter approach is stated in a *lagrangian* reference and within the elastic range. A finite elements algorithm was written for the governing system of equations within FlexPDE software environment (PDE Solutions Inc., 2009). The main statement of the finite deformations elastic model is outlined next.

Finite deformations elastic model: Equations of motion and constitutive law. Since the problem is stated in the *lagrangian* , or material reference, only the following equation has to be approximated, $\nabla_X \cdot \mathbf{P} + \rho_0 \mathbf{b} = \rho_0 \mathbf{A}$. $\mathbf{P}$ is the first Piola-Kirchhoff stress tensor, $\rho_0 = \rho(\mathbf{X}, t_0)$ is the mass density of the initial configuration, $\mathbf{A} = \dot{\mathbf{V}} = \partial \mathbf{V}/\partial t = \partial^2 \mathbf{x}/\partial t^2$ is the acceleration field, $\mathbf{b}$ are the body forces and, $\mathbf{x} = \mathbf{x}(\mathbf{X},t)$ is the spatial position vector. ∇_X or $\nabla_X \cdot$ represents the gradient and the divergence with respect to the material coordinates $\mathbf{X}$. Within this frame, the boundary conditions are imposed on the initial boundary whose position is known by hypothesis: $\mathbf{x}(\partial V^1) = \bar{\mathbf{x}}$, $\mathbf{t}_0(\partial V^2) = \bar{\mathbf{t}}_0$. $\mathbf{t}_0$ is the tension vector of Piola - Kirchhoff calculated for the rule $\mathbf{t}_0 = \mathbf{P} \cdot \mathbf{N}$. Thus, the problem at the boundary, as well as the initial conditions and the equations of motion, are fully stated. Once the differential problem is approximated, both, the position of the boundary and the location of any part of the body, will be known for each instant. The second Piola-Kirchhoff stress tensor may also be useful. As is known, it is symmetric and is given by $\mathbf{P} = \mathbf{F}\mathbf{S}$ where $[\mathbf{F}]_{ij} = \partial x_i/\partial X_j$ is the deformation gradient tensor, x_i is the ith component of the current position vector (spatial description), X_j is the jth component of the reference position vector (material description), $\mathbf{X}$. Then, the equations of motion can be rewritten as $\nabla_X \cdot (\mathbf{F}\mathbf{S}) + \rho_0 \mathbf{b} = \rho_0 \mathbf{A}$. The relationship $\mathbf{F} \cdot \mathbf{S} = (\det \mathbf{F}) \, \sigma \, (\mathbf{F}^{-1})^T = \mathbf{P}$ relates $\mathbf{P}$, $\mathbf{S}$ and σ (the Cauchy stress tensor—spatial description). Regarding the constitutive law, in this work we will deal with elastic materials which satisfy $\mathbf{S} = g(\mathbf{E})$ were g is a certain tensorial function, $[\mathbf{E}]_{ij} = \frac{1}{2} \left(\frac{\partial u_i}{\partial X_j} + \frac{\partial u_j}{\partial X_i} + \frac{\partial u_k}{\partial X_i} \frac{\partial u_k}{\partial X_j} \right)$ is the *lagrangian* finite strain tensor (also known as Green-St. Venant) and $\mathbf{u} = \mathbf{x}(\mathbf{X},t) - \mathbf{X}$ is the displacement vector. In particular, the following constitutive law is proposed: $\mathbf{S} = \lambda \, tr(\mathbf{E})\mathbf{I} + 2\mu\mathbf{E}$ where λ and μ are constants. This law is also known as St. Venant–Kirchhoff material model.

Contact model. As a first approach to the contact model, let us suppose that a deformable body interacts with a rigid and fixed obstacle. The contact condition is that the deformable
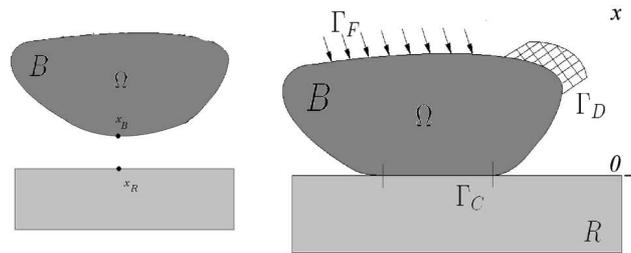
Figure 12: Scheme of the contact of a deformable body against a rigid contact.

body does not penetrate in the rigid obstacle. Let a body B occupy the domain Ω in a two- or three-dimensional space (Fig. 12). The body boundary $\Gamma = \Gamma_F \cup \Gamma_D \cup \Gamma_C$ is smooth enough and is in contact with a rigid fixed body. Part Γ_F of the boundary Γ corresponds to the boundary region at which the stresses are prescribed (natural conditions). Γ_D is the region where the displacements are prescribed (geometric conditions) and Γ_C, where there is contact with the rigid body. There, the displacements $\mathbf{v} = \mathbf{x}_B - \mathbf{x}_R$ are the difference between the coordinate of the point at the deformable body boundary and the corresponding one at the rigid boundary (see Fig. 12). The Signorini problem (unilateral contact) is stated as $v_N \leq 0$; $t_{cN} \leq 0$; $v_N t_{cN} = 0$ (subscript N denotes the normal direction; v_N is the normal component of $\mathbf{v}$ and t_{cN} is the contact force in the normal direction). Thus, there is **no contact** when $v_N \leq 0$ and $t_{cN} = 0$ and there is **contact** when $v_N = 0$ and $t_{cN} \leq 0$. These conditions constitute a non-continuous or non-smooth problem since tc_N is a multi-valuated application of the v_N field (or simply, tc_N is not a function of v_N). An alternative to solve this problem is a regularization by replacing the rigid condition by a smooth or regular one. The non-holonomic problem is replaced by a problem without constrain. The boundary condition will be always natural, by imposing a functional relationship between stresses and displacements. i.e. the problem is regularized by means of the following function: $t_{cN} = -k (v_N)^m$ if $v_N > 0$ or $t_{cN} = 0$ if $v_N \leq 0$ where k is a sufficiently large number in order to approximate the non-smooth problem and m is an arbitrary constant ($m = 1$ for the linear approximation). After some studies, the value of k was assumed as 100 times the numerical value of E. This problem can be extended to the contact between two deformable bodies. When dealing with infinitesimal strains and displacements, the contact problem is easily approximated by introducing a change of variable in the Signorini problem which is now double. That is, when dealing with body B1, $d(x_1, x_2) \geq 0$, $t_{cN1} \leq 0$ and $x_1 t_{cN1} = 0$. Regarding body B2, $d(x_2, x_1) \geq 0$, $t_{cN2} \leq 0$ and $x_2 t_{cN2} = 0$. $d(x_1, x_2)$ and $d(x_2, x_1)$ are both the distance between x_1 (B1) and x_2 (B2). When infinitesimal displacements are assumed, then unit vectors satisfy $\mathbf{N}_2 = -\mathbf{N}_1$ and the pair of points x_1 and x_2 are known before the problem is approximated, and are located on the normal to each surface. Instead, if the displacements or strains are considered finite, there is no knowledge about which pair of points will contact, neither about the corresponding normal unit vectors. In this case, the minimum of the distances between all possible pair of points have to be evaluated as well as the corresponding unit normal vectors.

Interaction force and time of contact. After solving the elasticity problem the fields are known. If V_0 is the non-deformed volume of the body, the acceleration of the center of mass can be calculated as $\mathbf{A}_{CM} = \frac{1}{V_0} \int \int \int \mathbf{A}(\mathbf{X}, t) \, dV_0$. The interaction force function then results $\mathbf{F}(t) = \int \int \int \mathbf{A}(\mathbf{X}, t)\rho_0 \, dV_0$.

The time of contact is the time during which the interaction force is not null.

Two situations will be examined. First, the modulus of elasticity is assumed to be the only random variable of the first model. Both small and large deformations will be considered and the previsions of both models will be compared. Second, the modulus of elasticity and the Poisson's coefficient will be supposed random, hence two random variables are involved in the second model.

The large deformation problem is approximated through the finite elasticity equations discretized via finite elements; details can be found in (Buezas et al., 2010).

5.1 One stochastic parameter. Small and large deformations.

Within the Hertz theory, the linear elastic model is not governed by a relationship as simpler as the one corresponding to the spheres problem (Eq. (13)). According to Puttock and Thwaite (1969), the equation that relates the interaction force and the interpenetration (total displacement of the mass centers) is,

$$x = \frac{F}{a} \left(\frac{1 - \nu^2}{\pi E} \right) \left[1 + \ln \left(\frac{8a^3 \pi E}{(1 - \nu^2) F r} \right) \right]. \tag{14}$$

The disc radius is $r = 1$, the mass density is $\rho = 2500$ and the thickness is $2a = 2$. All the values are measured in the S.I. units. Since it is very hard, if not impossible, to obtain an explicit expression of the force by direct inversion, an implicit differential equation has to be approximated to produce the inverse numerically. Additionally, no closed algebraic simple solution exists for the time of contact as function of the impact speed analogous to Eq. (1) of the spheres case. Consequently, Eq. (14) is approximated numerically. Two cases will be studied: a linear case (small deformations, low impact speed) and a non-linear case (larger deformations, higher impact speed). As before, a gamma PDF was derived for the variable E. A typical mean value of the modulus of elasticity for rubbers will be employed: $E = 5\,10^9\,Pa$. The Poisson coefficient is assumed deterministic with a value $\nu = 0.3$. Equation 14 together with the second Newton's law permits the approximation of the problem by Monte Carlo simulation. The distributions of the time of contact obtained from the propagation of the uncertainty in the modulus of elasticity are shown in Fig. 13 for a value of impact speed of 10 m/s and a dispersion $\sigma = 10^9$ Pa found with Monte Carlo simulations and 2000 realizations. Also, a convergence study was carried out to determine the appropriate number of realizations and it is shown in Fig. 14. It can be observed that with 2000 realizations a reasonable convergence of the results is obtained.

Since the Hertz theory assumes small deformations, it is not valid when larger deformations are involved. In this case, a finite deformation model is employed using the theory of Finite Elasticity discretized by finite elements. Large deformations are obtained for an impact speed of 100 m/s. Figure 15 includes the distributions of the modulus of elasticity and the time of contact found with the small and large deformations theories, respectively. From them, it can be observed that the propagation of the uncertainty to the time of contact is larger for the large deformations case where the dispersion results to be $\sigma_\tau = 1.94\,10^{-7}$ while in the linear case the result is $\sigma_\tau = 1.52\,10^{-7}$s. Figure 16 compares the distributions on the time of contact obtained for the two cases, using the *ksdensity* MATLAB routine, as before. It can be seen that the higher impact speed problem is not adequately modeled with the Hertz theory, as expected.
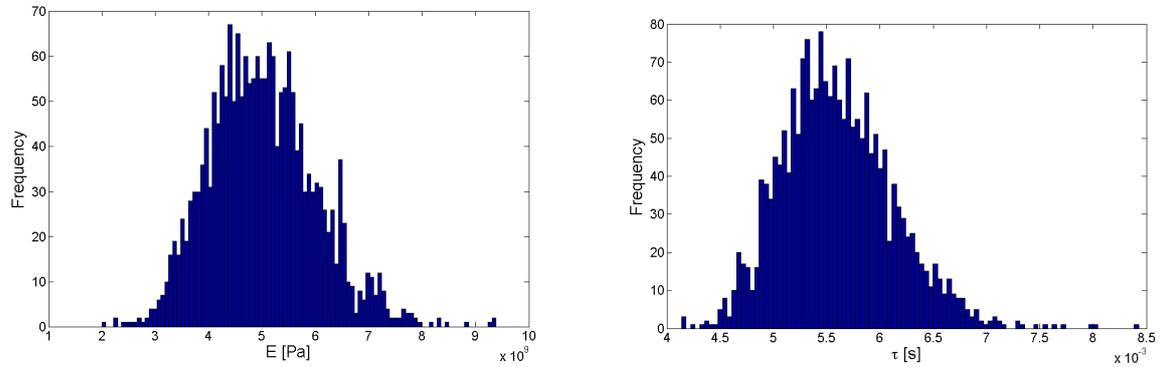
Figure 13: Collision between two discs. Histograms found with Monte Carlo simulations and 2000 realizations. Small deformation case. Left graph: modulus of elasticity; right graph: time of contact.
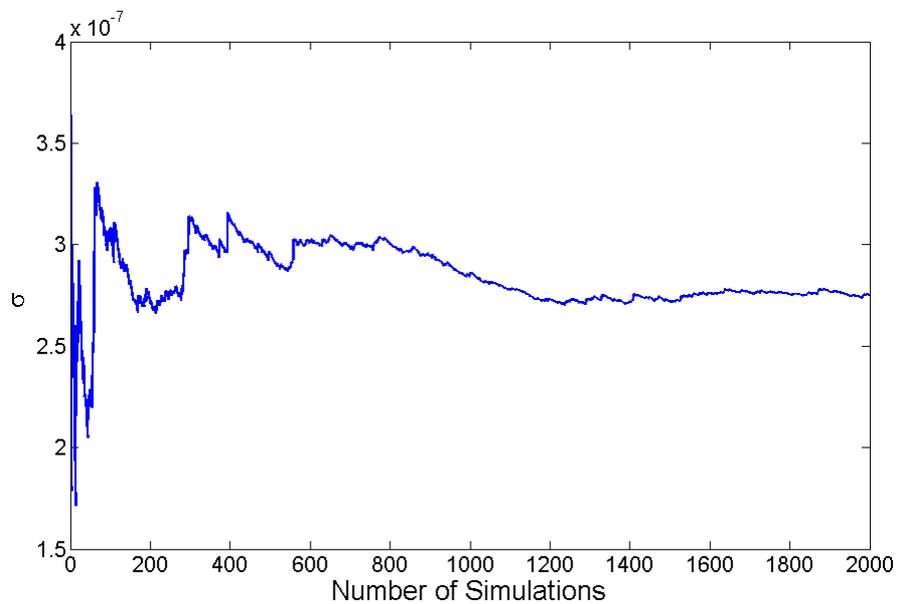

Figure 14: Collision between two discs. Convergence study of the standard deviation of the time of contact with Monte Carlo simulations.
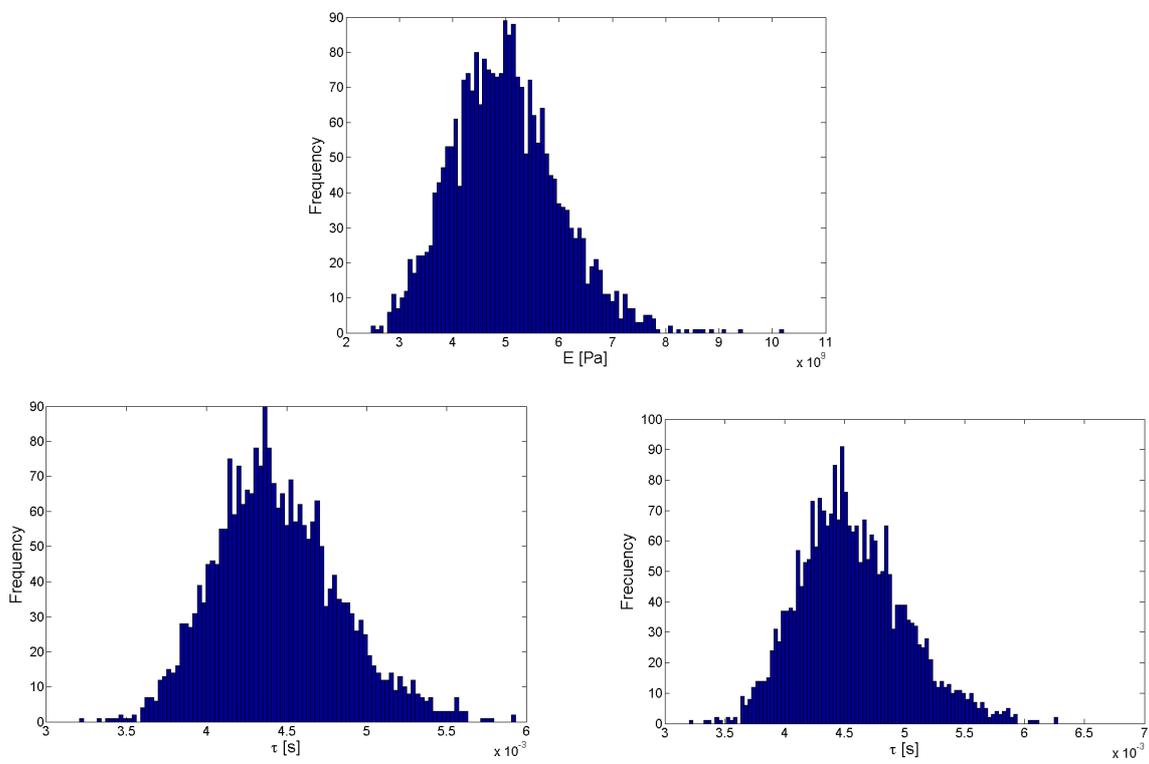
Figure 15: Collision between two discs. Histograms found with Monte Carlo simulations and 2000 realizations. Top graph: modulus of elasticity; lower left graph: time of contact for the small deformations example ($v = 10$ m/s) ; right graph: time of contact for the large deformation example ($v = 100$ m/s).
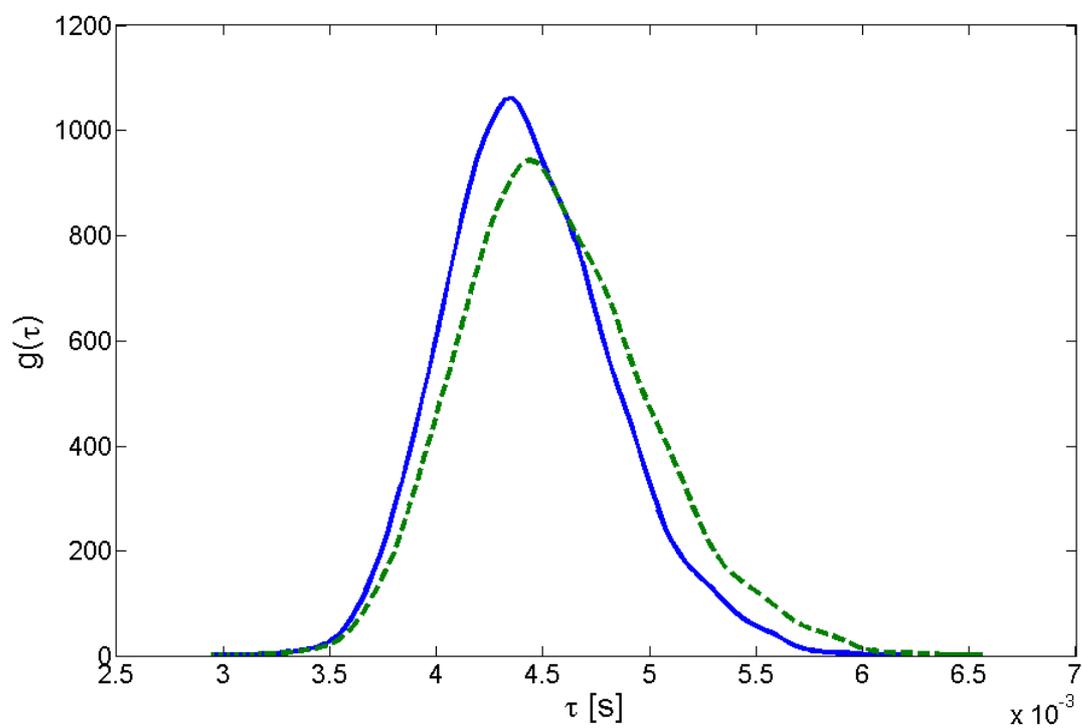
Figure 16: Collision between two discs at $v = 100$ m/s. Reconstruction of the time of contact PDFs from the numerical simulations using Monte Carlo method reconstructed from data of the lower graphs of Fig. 15. Full line: result from the linear theory; dashed line: result from the finite deformation theory.
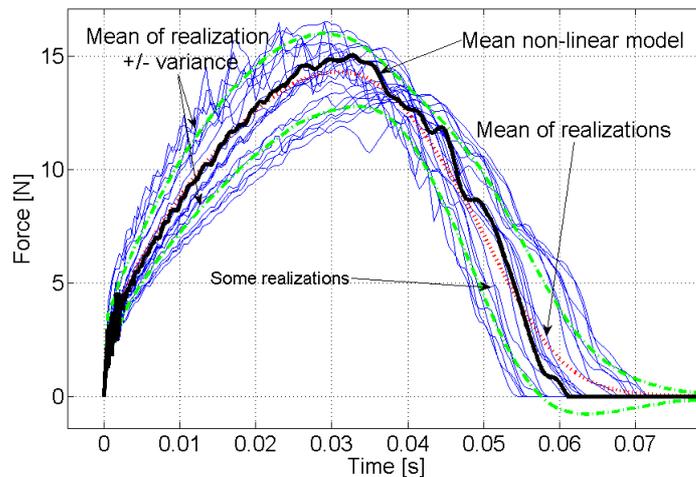
Figure 17: Temporal variation of the contact force. Case 1. Modulus of elasticity E(gamma PDF) $\mu_E = 1 \ 10^7$ Pa. $\sigma_E = \mu_E/5$. Poisson's ratio with uniform PDF. Some randomly chosen realizations (blue full lines), mean of the realizations (dashed red) and the simulation of the mean problem (black full line).

5.2 Two stochastic parameters. Large deformations.

The collision of the two discs is now studied in the range of large deformations, solving the Finite Elasticity problem via a finite element discretization. Two parameters are simultaneously assumed stochastic: the modulus of elasticity and the Poisson's ratio. As before, the PDF distribution for the modulus of elasticity is derived from the application of the PME. Thus, and under the restriction of positiveness, a gamma PDF is obtained. As is known, the Poisson's coefficient for the standard materials is bounded between 0 and 0.5. Then, if this is the only information available on the stochastic variable, the application of the PME yields a uniform PDF in that range. A numerical illustration is carried out assuming the collision of two discs made of a soft rubber, of the same mass density $\rho = 960$ kg/m3. The number of realizations was of 1250 for discs of radius $r = 0.1$ m, thickness $a = 0.01$ m that collide at $v = 1$ m/s. The modulus of elasticity E and the Poisson's ratio ν are assumed stochastic. The gamma PDF for E is assumed with mean $\mu_E = 1 \ 10^5$ Pa and a uniform distribution for ν within the range $[0, 0.5]$, i.e. $\mu_\nu = 0.25$. Of course, as already stated, in the finite elasticity approach one deals with a continuum. In order to calculate the interaction force function, a mean acceleration $\ddot{x}$ is first obtained and then all the forces integrated throughout the domain.

5.2.1 Two disc collision. Two stochastic parameters. Case 1

The collision is simulated for the problem described at the beginning of Subsection 5.2. Here the dispersion of parameter E is assumed $\sigma_E = \mu_E/5$.

Figure 17 shows the temporal variation of the interaction force (only a few realizations randomly chosen from the total of 1250, are depicted). Also, the mean of the realizations (dashed red) and the simulation of the mean problem (i.e. the problem approximated with the mean values of the stochastic parameters) (black full line) are plotted. As expected, the two latter curves do not coincide. Additionally, two green dashed lines found with $\mu \pm \sigma$, respectively. It is observed that the lower green curve is not valid at the end of the studied interval since no negative force is admissible. In this problem, adhesion was not considered and consequently, traction *negative* forces are not possible. These $\mu \pm \sigma$ curves make sense when dealing other
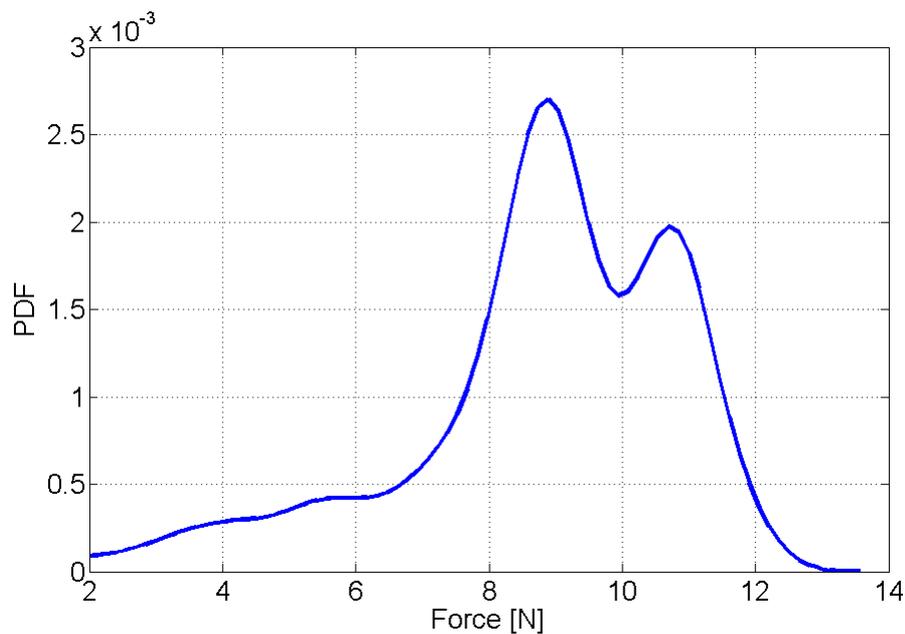
Figure 18: Idem Fig.17. Probability density function of the interaction force at $t = 0.0475$s. Bimodal distribution.

types of PDF, like a Gauss distribution. Here, they represent arbitrary bounds. In Fig. 17 a narrowing of curves region is observed around $t = 0.0475$ s, after the beginning of the impact. If the PDF of the force is constructed for this particular instant, a particular phenomenon is observed (Fig. 18). The PDF exhibits a bimodality. If a previous instant is observed, only one mode is observed. The phenomenon can be best depicted in the evolution of the PDF plotted in Fig. 19. The folding of the surface is evident after the interaction force reaches its maximum value. Then, this qualitative change may be regarded as a stochastic bifurcation.

The autocorrelation function $R(k) = E[(X_i - \mu)(X_{i-k} - \mu)]/\sigma^2$ is another interesting statistical measure where E stands for the expected value and k is the considered time displacement (sometimes named lag). Here, the interaction force is found at every pair of instants (t_i, t_{i-k}). As is known, this function varies within the range $[-1, 1]$ indicating the degree of linear dependence, where 1 denotes a perfect correlation and -1, perfect anti-correlation. As it approaches zero, the force is closer to uncorrelated. As the coefficient tends to -1 or 1, the stronger the correlation between the stochastic variables. If the variables are independent, the coefficient is 0, although the converse statement is not true. Figure 20 shows the autocorrelation of the interaction force for Case 1. The blue and red regions depict the values -1 and 1 respectively. Again, the region close to $t = 0.0475$ s exhibits a region of a narrow positive correlation. This is related to the observed narrowing of the dispersion curves of Fig.17.

5.2.2 Two disc collision. Two stochastic parameters. Case 2

The same problem approximated as Case 1 is herein tackled assuming a standard deviation value $\sigma_E = 2\mu_E/5$ *i.e.* twice the dispersion value assumed in Case 1. All the other data remain unchanged. Some of the realizations are shown in Fig. 21. As before, the mean of the simulations and the simulation of the mean problem are also plotted. As the dispersion of the modulus of elasticity is increased, the dispersion of the curved at the bottleneck close to $t = 0.0475$ s is higher. This expected result yields a smoothing of the two peaks of the force PDF as shown in Figs. 22 and 23. Compare with the previous case corresponding plots Figs.
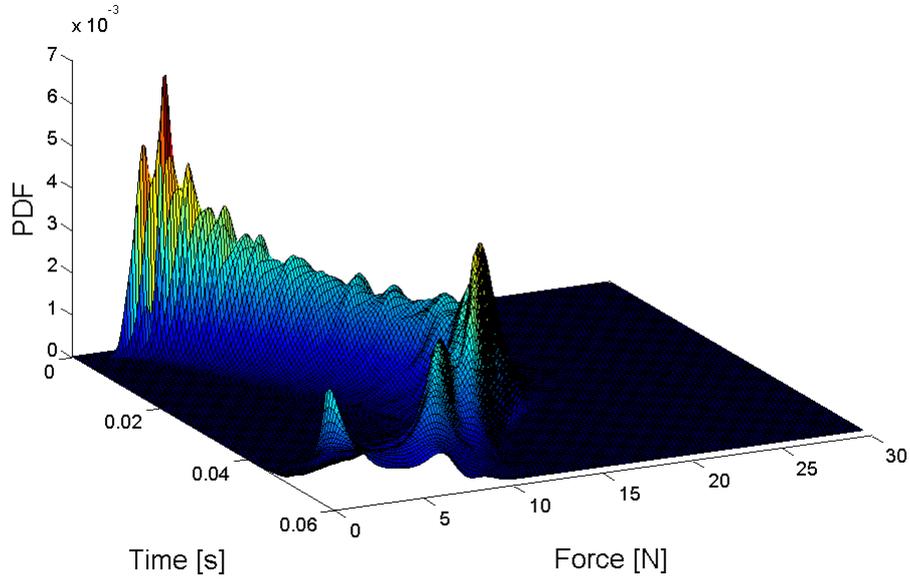
Figure 19: Idem Fig.17. Evolution of the probability density function of the interaction force.
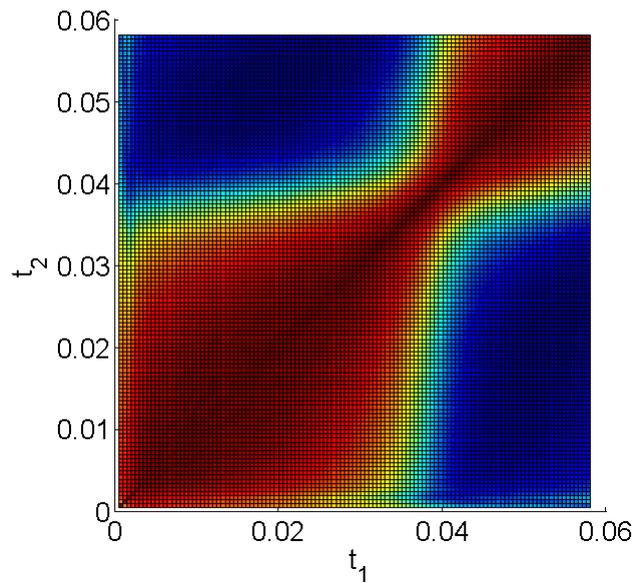

Figure 20: Idem Fig.17. Autocorrelation coefficient. Blue color corresponds to the value -1 (fully anticorrelated). Red color corresponds to the value 1 (fully correlated).
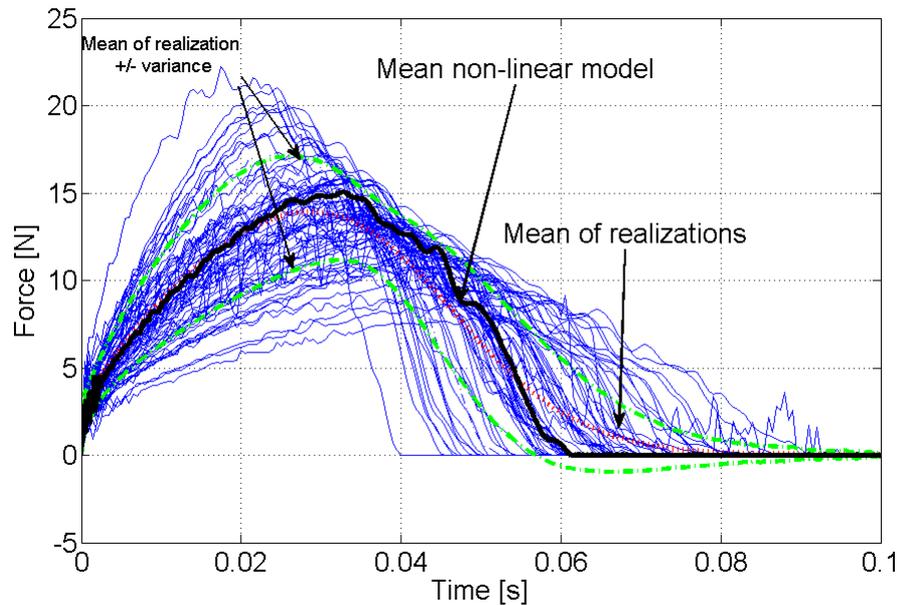
Figure 21: Temporal variation of the interaction force. Case 2. Modulus of elasticity E(gamma PDF) $\mu_E = 1e7$ Pa. $\sigma_E = \mu_E/5$. Poisson's ratio with uniform PDF. Ten random realizations (blue full lines), mean of the realizations (dashed red) and the simulation of the mean problem (black full line).

18 and 19. Also, as expected, the autocorrelation function (Fig. 24) exhibits a widening of the bottleneck at $t = 0.0475$ s (*Cf.* with Fig. 20).

Although not shown herein, other cases with this and other geometries, show multimodal PDF representing the interaction force. An observed trend is that for smaller dispersion, the multimodality (bimodality in the present illustrations) becomes more evident.

6 FINAL COMMENTS

The study addressed the collision of two elastic bodies. First, the case of two spheres was analyzed with the Hertz theory (small deformations) and using an analytic approach. One parameter involving material and geometric properties was assumed stochastic and the propagation of the uncertainty was studied. The Principle of Maximum Entropy stated in 1948 by Shannon is a means to select the most appropriate PDF for the stochastic parameter under the known information. Also, the same problem was approximated via a stochastic solver using Monte Carlo method. Then, probability density functions and confidence regions were obtained for the time of contact and the interaction force function. An interesting comparison between the numerical simulations and the analytical results was possible in this case. It is concluded that the Monte Carlo method exhibits robustness. This method can always be applied since in fact, it is the simulation of a real physical experiment. When the stochastic dimension of the problem is one, *i.e.* there is only one stochastic parameter, it would be always possible to construct a numerical functional relationship between the input and the output variables, and then apply the change of variable technique shown at the beginning of this article. Having this tool, 10 to 50 runs would suffice to construct the derived PDF. Clearly, when we deal with larger stochastic dimension problems (more stochastic variables), the change of variables would involve a Jacobian transformation and the number of simulations would increase as powers of the dimension. Here, the Monte Carlo method, or a similar one, would be advantageous. It should be noted that the interaction force is derived from a non-linear differential equation. The second prob-
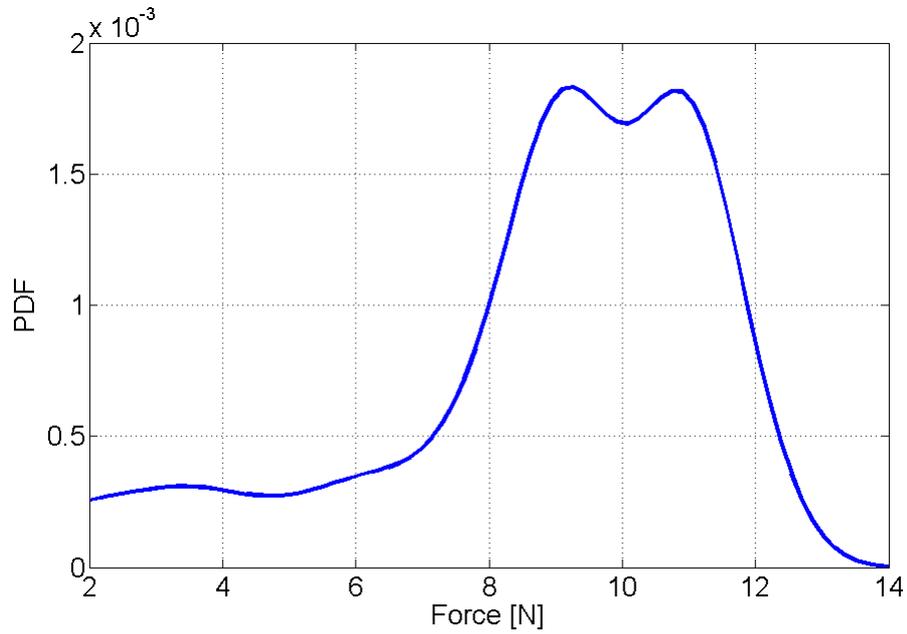
Figure 22: Idem Fig.21. Probability density function of the interaction force at $t = 0.0475$ s.
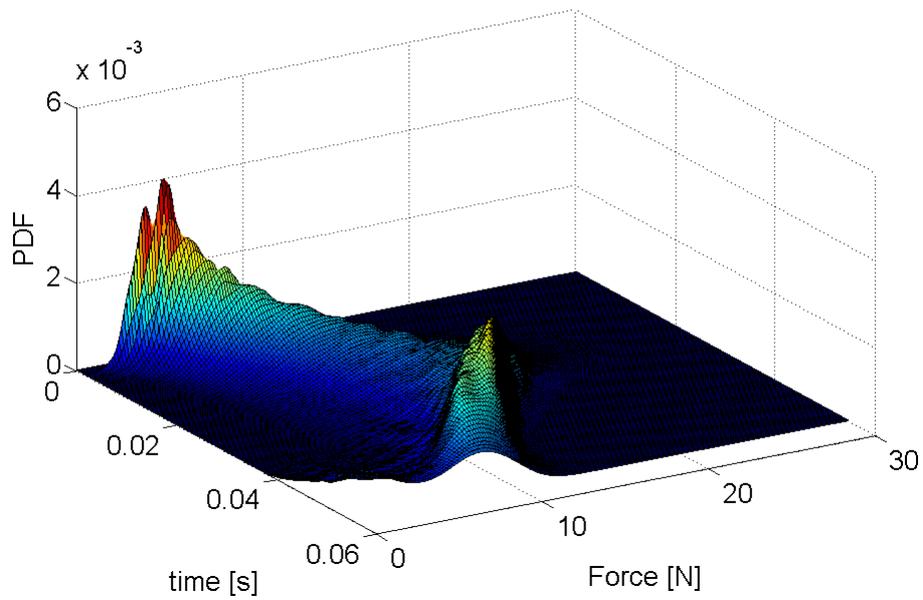

Figure 23: Idem Fig.21. Evolution of the probability density function of the interaction force.
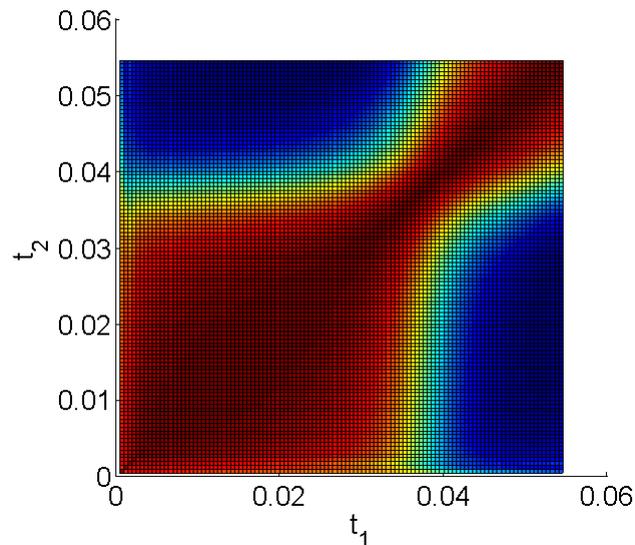
Figure 24: Idem Fig.21. Autocorrelation coefficient. Blue region corresponds to the value -1 (fully anticorrelated). Red region corresponds to the value 1 (fully correlated).

lem studied deals with the collision of two discs. Two situations were first addressed, low and high impact speed and a rather soft material (rubber), assuming the modulus of elasticity E as a statistical variable. In the first case, the linear Hertz theory is applicable since one supposes small deformations. On the other hand, when the speed is higher, it is shown that it is necessary to use a finite deformation scheme to solve the elastic collision problem. It should be noted that when dealing with discs there is no explicit relationship between the time of contact τ and impact speed, neither in the Hertz model nor in the finite elasticity solution. Hence, the analytical approach is not feasible and a numerical procedure is the alternative. Later, the uncertainty quantification was performed in the two discs collision problem by assuming two stochastic parameters, the modulus of elasticity E and the Poisson's ratio ν. A gamma PDF was derived for E and a uniform PDF for ν. Additionally, the dispersion of E was taken with two possible values. Several graphs allowed to observe some particular phenomenon around the instant $t = 0.0475$ s. In certain cases, specially when the dispersion of the stochastic variables assumes the smaller values, a qualitative change is present in the PDF distribution of the force. In effect, in Case 1, a bimodal PDF is obtained at this instant, which is not present in the whole interval. The temporal variation of the interaction force plots show that, after the maximum value of the force is attained, there is a narrowing of the region where the statistical realizations are located and this is reflected in the three-dimensional plot of the evolution of the force. This effect is more evident with lower dispersion values of the stochastic parameters and the PDFs undergo bifurcations exhibiting two modes at a particular instant. On the contrary, increasing the dispersion appears to have an averaging effect on the PDFs.

The collision problem, when dealing with large deformations, is not symmetrical with respect to time reversal. Since the bodies are bounded, at the instant of collision, compression waves travel the bodies and once they reach boundaries they are reflected as elastic waves, these reflections continue until the end of the collision. The reflected waves change the stress field in the bodies and causes the non-symmetry. To explain the multimodality is more complex and one possible explanation is in the reference (Pagnacco et al., 2011). The problems treated in this paper are conservative and can not represent exactly a real collision, also only the simplest

case of collision was treated, the frontal collision. The greatest uncertainty in the collision is the type of collision, if frontal or not. If it is not frontal the situation is much more complex as one can see in (Stronge, 2000; Cataldo and Sampaio, 2002). It is also important to remark that rigid collision is completely different from elastic collision or from plastic collision. The constitutive equation used for the rubber is not the best one but it simplifies the problem. Even with all this assumptions, the problem is hard and one needs to solve a complex finite elasticity problem to get the results.

At present, more cases involving large deformations and elastic bodies of arbitrary geometry are being studied as well as the introduction of friction and dissipation. The hope is to construct a deterministic theory of collision for large deformations that allows the construction of a good stochastic model.

7 ACKNOWLEDGEMENTS

8 REFERENCES

Buezas F., Rosales M., and Filipich C. Collisions between two nonlinear deformable bodies stated within continuum mechanics. *International Journal of Mechanical Sciences*, 52(6):777–783, 2010.

Cataldo E. and Sampaio R. A new model of rigid bodies collision: the c-s model. *Computational and Applied Mathematics*, 19(3):349–362, 2000.

Cataldo E. and Sampaio R. A brief review and a new treatment for rigid bodies collision models. *Journal of the Brazilian Society of Mechanical Sciences*, 23(1):63–78, 2001a.

Cataldo E. and Sampaio R. Comparación entre modelos de colisión de cuerpos. *Revista Internacional de Métodos Numéricos para Cálculo y Diseño en Ingeniería*, 17(2):149–168, 2001b.

Cataldo E. and Sampaio R. Modelagem e simulação de colisões entre corpos rígidos. *Revista Internacional de Métodos Numéricos para Cálculo y Diseño en Ingeniería*, 18(1):111–192, 2002.

Hessel R., Perinotto A., Alfaro R., and Freschi A. Force-versus-time curves during collisions between two identical steel balls. *American journal of physics*, 74:176, 2006.

Johnson K.L. *Contact Mechanics*. Cambridge University Press, 1985.

Landau L. and Lifchitz E. *Física teórica. Teoría de la Elasticidad*, volume 7. Reverte Editorial SA, 1969.

Langley R. The analysis of impact forces in randomly vibrating elastic systems. *Journal of Sound and Vibration*, 331(16):3738 – 3750, 2012.

Pagnacco E., Sampaio R., and Souza de Cursi J.E. Frequency response functions of random linear mechanical systems and propagation of uncertainties. In *ENIEF 2011*, volume XXX, pages 3357–3380. Rosario, Argentina, 2011.

PDE Solutions Inc. *FlexPDE software*. 2009.

Pérez A. *Problemas de máxima entropía*. Master's Thesis, Universidad Central de Venezuela, 2007.

Popov V.L. *Contact Mechanics and Friction*. Springer, 2010.

Puttock M. and Thwaite E. *Elastic compression of spheres and cylinders at point and line contact*. Commonwealth Scientific and Industrial Research Organization, 1969.

Ritto T., Buezas F., and Sampaio R. Proper orthogonal decomposition for model reduction of a vibroimpact system. *Journal of the Brazilian Society of Mechanical Sciences*, to appear, 2012.

Ritto T., Lopez R., Sampaio R., and Souza De Cursi J. Robust optimization of a flexible rotor-bearing system using the Campbell diagram. *Engineering Optimization*, 43(1):77–96, 2011.

Rubinstein R.Y. *Simulation and the Monte Carlo Method*. Series in Probability and Statistics. John Wiley and Sons, New Jersey, USA, 2nd edition, 2007.

Sampaio R. and Soize C. On measures of nonlinearity effects for uncertain dynamical systems– application to a vibro-impact system. *Journal of Sound and Vibration*, 303(3–5):659–674, 2007.

Sampaio R. and Tavares H.M. Colisão em sistemas de multicorpos rígidos. *Journal of the Brazilian Society of Mechanical Sciences*, 20(1):116–125, 1998.

Shannon C. A mathematical theory of communication. *The Bell Technical Journal*, 27:379–423, 1948.

Spiegel M. *Probability and Statistics*. Schaum. McGraw–Hill, 1998.

Stronge W.J. *Impact Mechanics*. Cambridge University Press, 2000.

Timoshenko S. Zur Frage nach der Wirkung eines Stosses auf einen Balken. *Zeitschrift fur Mathematik und Physik*, 63:198–209, 1913.